scientific reports

Check for updates

OPEN

Adipose-derived stem cells using fibrin gel as a scaffold enhances post-hepatectomy liver regeneration

Hiroki Imamura[1], Yoshito Tomimaru[1], Shogo Kobayashi[1]✉, Akima Harada[2], Shunbun Kita[3,4], Kazuki Sasaki[1], Yoshifumi Iwagami[1], Daisaku Yamada[1], Takehiro Noda[1], Hidenori Takahashi[1], Daiki Hokkoku[1], Takeshi Kado[1], Keisuke Toya[1], Takahiro Kodama[5], Shigeyoshi Saito[6], Iichiro Shimomura[3], Shigeru Miyagawa[2], Yuichiro Doki[1] & Hidetoshi Eguchi[1]

We investigated the potential of adipose-derived stem cells (ADSCs) in preventing post-hepatectomy liver failure, emphasizing the necessity of direct administration using a scaffold. A fibrin gel scaffold was employed for ADSCs (gelADSC) to assess their therapeutic impact on liver regeneration in both in vitro and in vivo settings. Experiments were conducted on C57BL/6 mice with normal livers and those with chronic hepatitis. We also explored the role of extracellular vesicles (EVs) secreted by ADSCs in conjunction with fibrin gel. GelADSC showed sustained release of hepatocyte growth factor, vascular endothelial growth factor, and stromal cell–derived factor 1 for at least 7 days in vitro. In vivo, gelADSC significantly enhanced postoperative liver regeneration by upregulating the cell cycle and fatty acid oxidation in both normal and chronically hepatitis-affected mice. The therapeutic effects of gelADSC were potentially favorable over those of intravenously administered ADSCs, especially in mice with chronic hepatitis. Increased EV secretion associated with fibrin gel use was significantly linked to enhanced liver regeneration post-surgery through the promotion of fatty acid oxidation. The findings underscore the enhanced therapeutic potential of gelADSC, particularly in the context of chronic hepatitis, possibly compared to intravenous administration.

Keywords Hepatectomy, Liver regeneration, Adipose-derived stem cell, Paracrine effect, Fibrin gel

Post-hepatectomy liver failure (PHLF) is a relatively rare but potentially life-threatening complication of hepatectomy. The incidence of PHLF is reported to range from 8 to 12%, with 2–10% mortality, depending on the volume of the resected liver[1]. Although liver transplantation is the only treatment for PHLF that is definitive and curative, it is potentially limited by donor availability and the invasiveness of surgery.

Adipose-derived stem cells (ADSCs) have shown promising tissue reparative properties in various types of organ dysfunction[2]. The two primary methods for administering ADSCs are intravenous injection and direct application to the affected organ. While intravenous injections are relatively simple and safe, they lack the ability to target ADSCs specifically to the damaged tissue. In contrast, direct administration allows for localized delivery of ADSCs to the injury site, but it requires a suitable scaffold to retain the cells at the target location. Therefore, determining the optimal route of ADSC administration is crucial when developing organ failure models.

Although ADSCs have been investigated as a potential preventive treatment for PHLF, most studies have focused on their intravenous administration[3]. Despite the promise of intravenous delivery, several limitations have been identified. Watanabe et al. reported that the majority of intravenously injected ADSCs become trapped in the lungs[4]. Moreover, there has been a report of pulmonary embolism, potentially linked to intravenous ADSC administration[5]. In contrast, some studies suggest that direct administration of ADSCs may offer superior

[1]Department of Gastroenterological Surgery, Graduate School of Medicine, Osaka University, 2-2 Yamada-oka, Suita 565-0871, Osaka, Japan. [2]Department of Cardiovascular Surgery, Graduate School of Medicine, Osaka University, Suita, Japan. [3]Department of Metabolic Medicine, Graduate School of Medicine, Osaka University, Suita, Japan. [4]Department of Adipose Management, Graduate School of Medicine, Osaka University, Suita, Japan. [5]Department of Gastroenterology and Hepatology, Graduate School of Medicine, Osaka University, Suita, Japan. [6]Department of Medical Physics and Engineering, Division of Health Sciences, Graduate School of Medicine, Osaka University, Suita, Japan. ✉email: skobayashi@gesurg.med.osaka-u.ac.jp

therapeutic benefits compared to intravenous injection[6]. In this context, Hu et al. highlighted the need to evaluate the most appropriate route of ADSC delivery for treating liver injury[7]. Thus, it is reasonable to explore the therapeutic potential of direct ADSC administration in a PHLF model, particularly using a scaffold to retain the cells at the liver surface.

To address this, we utilized fibrin gel (FG) as a scaffold for the administration of ADSCs for three main reasons. First, FG has been demonstrated to be an effective scaffold, providing a favorable environment for ADSCs without inducing their differentiation[8–11]. Second, FG is widely utilized in surgical practice to prevent bleeding and bile leakage following liver resection[12], making its safety and efficacy well-established in the context of hepatectomy. Third, due to its expandable nature, FG is particularly suited for covering the liver, a three-dimensional structure. In this study, we developed a mouse liver resection model to evaluate the therapeutic effects of ADSCs on liver regeneration by applying ADSCs to the liver surface, using FG as a scaffold.

Results

GelADSC displayed favorable survival and cytokine secretion in vitro

In this study, gelADSC refers to 1.0×10^6 ADSCs embedded in 2-fold diluted FG. First, we evaluated the in vitro dynamics of gelADSC. Histological examination of gelADSC cultured in vitro for 7 days revealed a considerable number of ADSCs within FG (Fig. 1a). TUNEL staining demonstrated a substantial population of viable ADSCs (Fig. 1b). Subsequently, the assessment of FG's influence on the secretion of vascular endothelial growth factor (VEGF), hepatocyte growth factor (HGF), and stromal cell-derived factor-1 (SDF-1) revealed consistently higher levels from gelADSC compared to those cultured without FG, and the levels of secreted cytokines continued to increase until day 7 (Fig. 1c). Furthermore, western blot (WB) analysis revealed that the expression of hypoxia inducible factor-1 α (HIF-1α) was heightened in the gelADSC group on days 3, 5, and 7 (Fig. 1d; the uncropped membrane is shown in Supplementary Fig. S1). These results suggest that gelADSC provided a favorable scaffold on which ADSCs were able to survive for at least 7 days, with the hypoxic condition potentially upregulating cytokine expression.

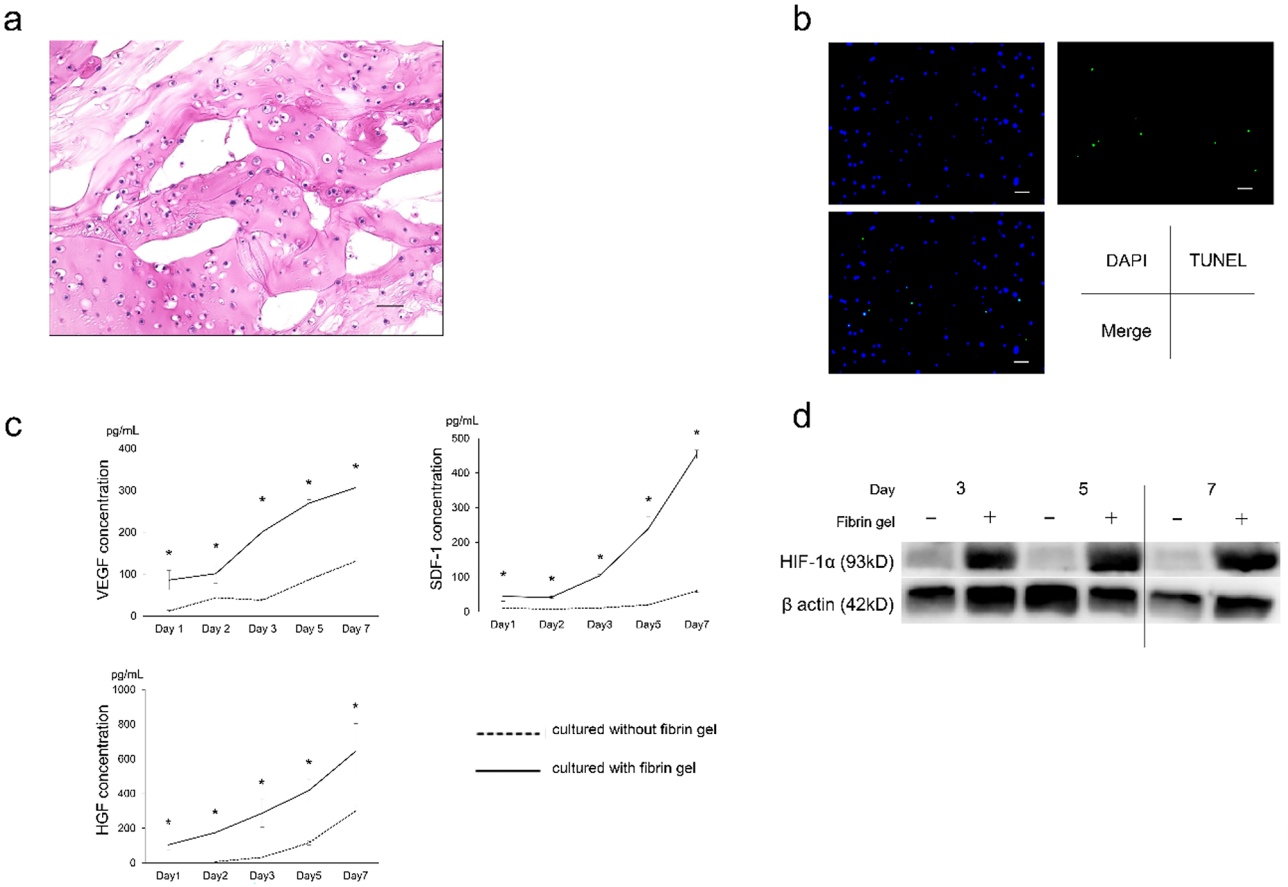

Fig. 1. In vitro evaluation of ADSCs embedded in fibrin gel. (**a**) H&E staining of gelADSC after 7-day incubation exhibited numerous ADSCs remaining in the fibrin gel. Scale bar = 50 μm. (**b**) TUNEL staining of gelADSC after 7-day incubation revealed viable ADSCs. Scale bar = 50 μm. (**c**) ADSCs embedded in fibrin gel (solid line) secreted significantly higher amounts of VEGF, HGF, and SDF-1 than did ADSCs incubated without fibrin gel (dotted line). (**d**) Western blot analysis showing the enhanced expression of HIF-1α by ADSCs embedded in fibrin gel on days 3, 5, and 7. *$p < 0.05$.

ADSCs survived in FG in hepatectomized mice

In the animal model using C57BL/6 mice, ADSCs were administered either embedded in FG (gelADSC group) or via intravenous injection (ivADSC group). Next, the dynamics of gelADSC in vivo were evaluated. GelADSC was extracted from hepatectomized mice on postoperative day (POD) 7. Histological analysis using hematoxylin & eosin (H&E) staining (Fig. 2a) and TUNEL staining (Fig. 2b) revealed that, similar to the in vitro results, the majority of ADSCs within FG remained viable in vivo on POD 7. Immunostaining of gelADSC revealed high expression of CD90 and CD105, which are known markers of ADSCs, and little expression of hepatocyte-specific antigen and arginase-1, which are commonly positive in hepatocytes (Fig. 2c). Furthermore, the in vivo distribution of ADSCs was assessed by labeling them with iron and tracking them by magnetic resonance imaging (MRI). Appropriate labeling was confirmed by Berlin staining (Fig. 2d). In the gelADSC group, FG on the liver surface was detected as a low-intensity signal on T2-weighted imaging (T2WI), reflecting the presence of iron (Fig. 2e). Notably, on PODs 1, 3, and 7, the liver exhibited a low-intensity signal on T2WI in the ivADSC group compared with the livers in the control group and the gelADSC group. Taken together, ADSCs remained within FG in hepatectomized mice for a duration of 7 days, demonstrating their undifferentiated status and continuous viability.

GelADSC promoted liver regeneration after hepatectomy in normal liver through upregulation of the cell cycle and fatty acid oxidation

In the gelADSC group, gelADSC was placed on the surface of the remnant liver after 70% partial hepatectomy (Fig. 3a). The remnant liver to body weight ratio (LTBR) significantly increased in the gelADSC group compared with the control group (mean: 0.034 vs. 0.029) on POD 2 (Fig. 3b). Immunostaining of proliferating cell nuclear antigen (PCNA) on thin sections of the liver on POD 2 showed a significant increase in PCNA-positive cells in the gelADSC group compared with the control group (Fig. 3c). Pathway analysis using RNA-seq revealed a significant upregulation of the cell cycle pathway in the gelADSC group (Supplementary Fig. S2a). H&E staining on POD 2 revealed less accumulation of lipid droplets in the gelADSC group (Fig. 3c). Cholesterol and triglyceride assays of liver samples demonstrated significantly lower triglyceride content in the gelADSC group compared with the control group, though the cholesterol level was comparable between the two groups (Fig. 3d). RNA-seq analysis revealed significant upregulation of fatty acid oxidation in the gelADSC group (Supplementary Fig. S2b). Polymerase chain reaction (PCR) analysis of mRNA extracted from liver samples showed significant upregulation of carnitine O-octanoyltransferase (Crot), carnitine palmitoyltransferase 1a

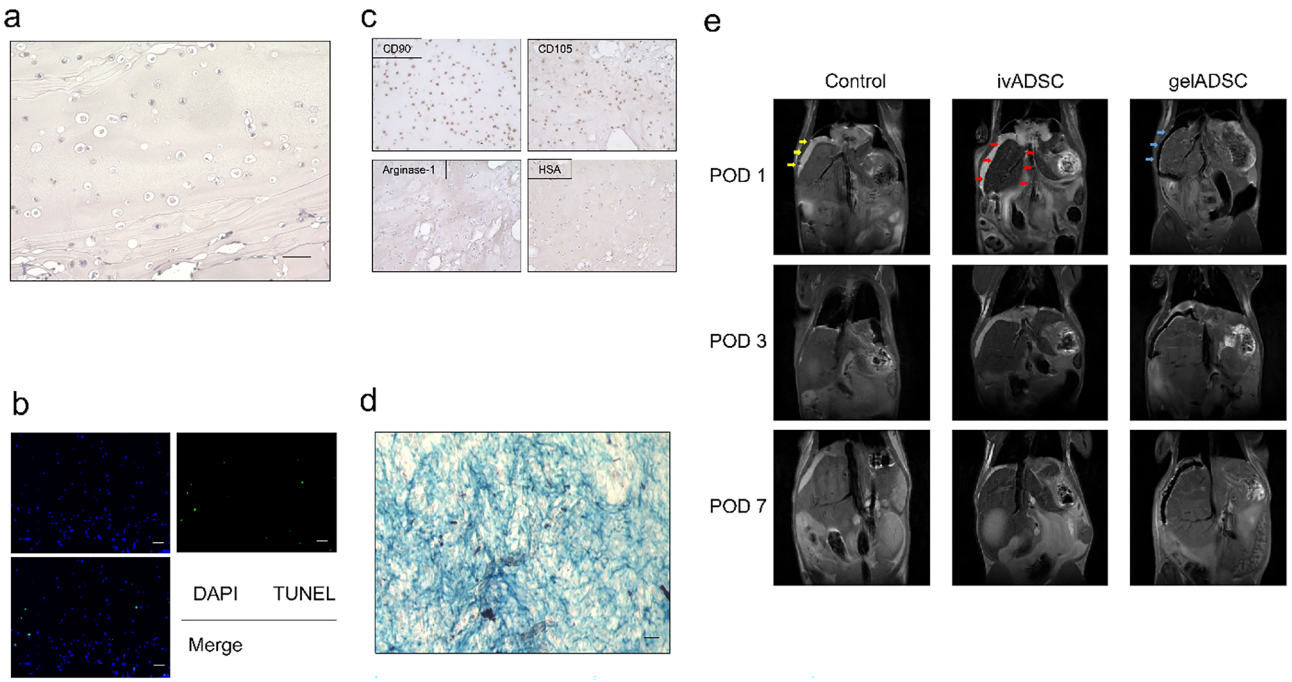

Fig. 2. In vivo evaluation of ADSCs embedded in fibrin gel. (**a**) H&E staining of gelADSC on postoperative day 7 revealed numerous ADSCs remaining in the fibrin gel. Scale bar = 50 µm. (**b**) TUNEL staining of gelADSC on postoperative day 7 revealed viable ADSCs. Scale bar = 50 µm. (**c**) Immunostaining of gelADSC using antibodies for CD90, CD105, arginase-1, and hepatocyte-specific antigen (HSA) revealed that ADSCs in the fibrin gel were diffusely positive for CD90 and CD105 but negative for arginase-1 and HSA. Scale bar = 50 µm. (**d**) Berlin staining of ADSCs confirmed labeling with iron. Scale bar = 50 µm. (**e**) The distribution of ADSCs in vivo was assessed by T2WI MRI. Fibrin gel exhibited a high-density signal on the liver surface (yellow arrows), whereas it exhibited a low-density signal when iron-labelled ADSCs were embedded in it (blue arrows). Intravenous administration (ivADSC) resulted in a hepatic distribution of ADSCs, as evidenced by the low-density liver parenchyma (red arrows).

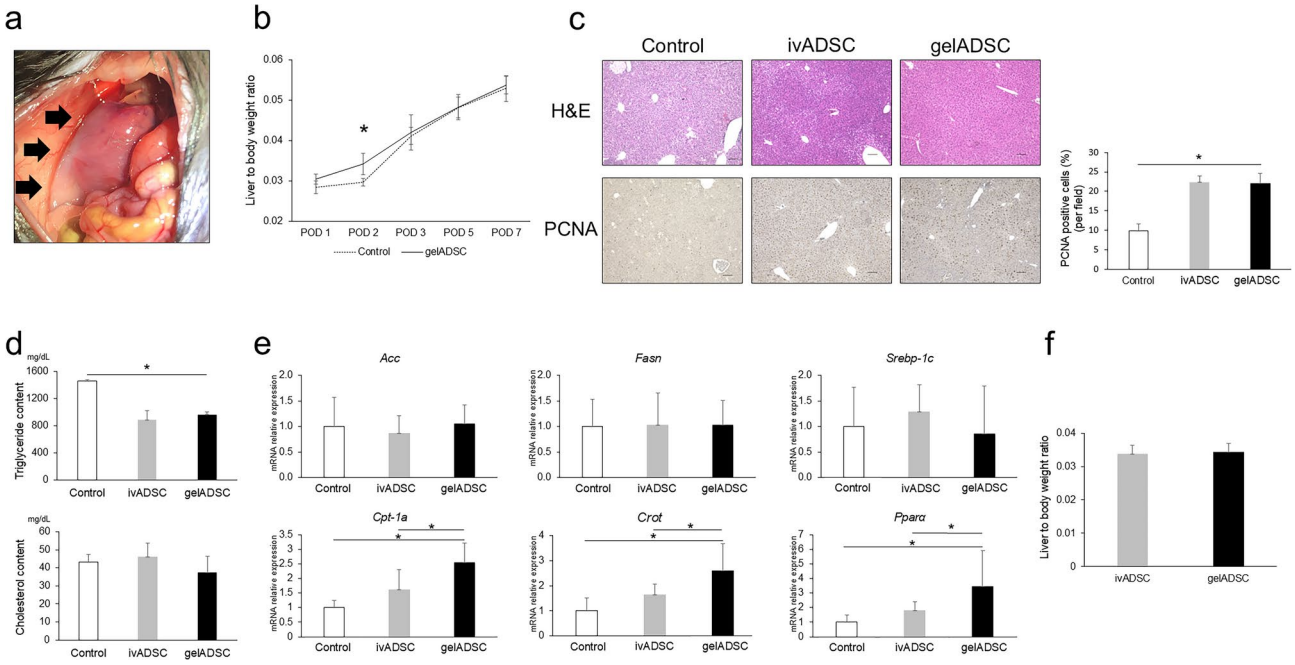

Fig. 3. Therapeutic effect of gelADSC after hepatectomy for normal liver. (**a**) Intraoperative photograph showing gelADSC placed on the surface of the remnant liver (black arrows). (**b**) The liver to body weight ratio was significantly higher on POD 2 in the gelADSC group than in the control group. (**c**) Representative images of the histological evaluation of remnant liver showing the accumulation of lipid in the control group on H&E staining, whereas such accumulation is decreased in the ivADSC and gelADSC groups. Immunohistochemistry for PCNA showed a significant increase in PCNA-positive cells in the gelADSC group compared with the control group. Scale bar = 100 μm. (**d**) A triglyceride assay revealed that the liver triglyceride content in the gelADSC group was significantly higher than in the control group but comparable to the ivADSC group. The cholesterol content was comparable between the three groups. (**e**) mRNA expression in the liver was evaluated by real-time PCR. The expression of Acc, Fasn, and Srebp-1c was comparable between the three groups, whereas that of Cpt-1a, Crot, and Pparα was significantly upregulated in the gelADSC group, the ivADSC group, and the control group in that order. (**f**) The liver to body weight ratio on POD 2 was comparable between the gelADSC group and the ivADSC group. $^*p < 0.05$.

(Cpt-1a), and peroxisome proliferator-activated receptor α (Pparα), which are involved in fatty acid oxidation, in the gelADSC group. In contrast, no significant differences were observed in the mRNA expression of acetyl-CoA carboxylase (Acc), fatty acid synthase (Fasn), and sterol regulatory element-binding protein 1c (Srebp-1c), which are involved in fatty acid synthesis (Fig. 3e). In addition, in the 90% hepatectomy model, the gelADSC group exhibited significantly improved survival compared with that of the control group ($p = 0.0013$; Supplementary Fig. S3). These comparisons between the gelADSC and the control groups highlighted the usage of gelADSC to enhance liver regeneration in the setting of hepatectomy for normal liver.

The therapeutic effect of gelADSC was further evaluated by comparing the gelADSC group and the ivADSC group. The LTBR on POD 2 was comparable between the two groups (mean: 0.033) (Fig. 3f). Histological analyses revealed that the number of PCNA-positive cells and the extent of lipid accumulation were also comparable between the two groups (Fig. 3c), as was the triglyceride content (Fig. 3d). In the ivADSC group, the expression of Cpt-1a, Crot, and Pparα mRNAs was significantly downregulated in comparison with that in the gelADSC group (Fig. 3e).

In summary, gelADSC contributed to post-hepatectomy liver regeneration by upregulating the fatty acid oxidation and cell cycle pathways. Moreover, the therapeutic impact of gelADSC seemed comparable to that of ivADSC, although the expression of mRNAs associated with fatty acid oxidation was possibly upregulated in the gelADSC group.

GelADSC promoted liver regeneration after 70% hepatectomy in liver with chronic hepatitis by upregulating the cell cycle and fatty acid oxidation

We investigated the therapeutic effects of gelADSC for hepatectomy in mice with chronic hepatitis. Five weeks of preoperative thioacetamide (TAA) administration successfully induced liver fibrosis, which was confirmed by Masson's trichrome staining (Fig. 4a). The LTBR did not differ significantly between the control group and the gelADSC group on PODs 1, 2, 5, and 7, but we did find a significant difference on POD 3 (mean: 0.034 vs. 0.037; $p = 0.0012$) (Fig. 4b). The LTBR was consistently lower than the values in hepatectomized mice with normal liver (Fig. 3b). H&E staining demonstrated reduced intracellular lipid droplets in the gelADSC group compared with the control group (Fig. 4c). Immunostaining for PCNA revealed an increase in the positive cells in the

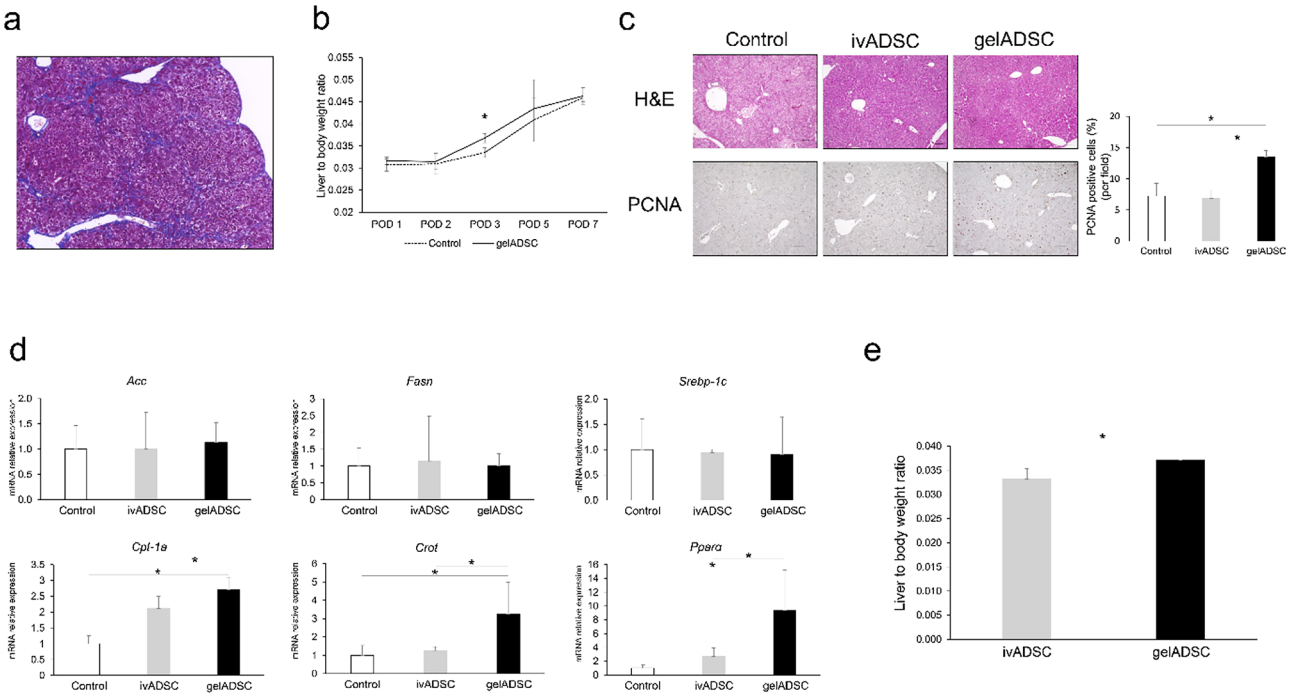

Fig. 4. Therapeutic effect of gelADSC after hepatectomy for chronic hepatitis. (**a**) Masson trichrome staining of the resected liver confirmed liver fibrosis. Scale bar = 100 µm. (**b**) The liver to body weight ratio gradually increased in both the control and the gelADSC groups, with a significant difference on POD 3 in favor of the gelADSC group, although the difference was not significant at PODs 1, 2, 5, and 7. (**c**) Representative H&E images of remnant liver demonstrating lipid accumulation in the control group, with less lipid accumulation in the ivADSC and gelADSC groups. Immunohistochemistry for PCNA showed a significant increase of PCNA-positive cells in the gelADSC group compared with the control and ivADSC groups. Scale bar = 100 µm. (**d**) mRNA expression in the liver was evaluated by real-time PCR. The expression of Acc, Fasn, and Srebp-1c was comparable between the three groups, whereas that of Cpt-1a, Crot, and Pparα was significantly upregulated in the gelADSC group compared with the control group and the ivADSC group. (**e**) The liver to body weight ratio at POD 3 was significantly higher in the gelADSC group than in the ivADSC group. $^{*}p < 0.05$.

gelADSC group compared with the control group (Fig. 4c). Furthermore, PCR analysis demonstrated significant upregulation of Cpt-1a, Crot and Pparα in the gelADSC group compared to the control group, although the expression of Acc, Fasn, and Srebp-1c was comparable between the two groups (Fig. 4d). The efficacy of gelADSC was also revealed in hepatectomy for chronic hepatitis liver by comparing it with the control group.

The therapeutic effect was further evaluated by comparing the gelADSC group with the ivADSC group. The LTBR on POD 3 significantly increased in the gelADSC group (mean: 0.033 vs. 0.037) (Fig. 4e). The histological analyses revealed that the number of PCNA-positive cells was increased in the gelADSC group, although lipid accumulation was comparable between the two groups (Fig. 4c). The mRNA expression of Cpt-1a, Crot, and Pparα was significantly increased in the gelADSC group (Fig. 4d).

In summary, gelADSC promoted post-hepatectomy liver regeneration by upregulating the cell cycle and fatty acid oxidation in the presence of chronic hepatitis. In this model, the therapeutic impact of gelADSC was superior not only to the control group but also probably to the ivADSC group.

The hepatic distribution of ADSCs administered through a tail vein decreased in the presence of chronic hepatitis

The post-hepatectomy distribution of ADSCs in a chronic hepatitis model mouse was evaluated by MRI. In the gelADSC group, FG containing iron-labeled ADSCs was consistently enhanced by a low-intensity signal for 7 postoperative days (Fig. 5a), just as it was after hepatectomy for normal liver (Fig. 2e). In contrast, in the ivADSC group, the liver did not display a low-intensity signal as it did after hepatectomy for normal liver. This finding was confirmed by the comparison of the liver signal intensity relative to that of muscle between the two ivADSC groups (i.e., the comparison between the ivADSC group mice with normal liver and those with chronic hepatitis). The signal intensity was significantly higher in the livers of the ivADSC group with chronic hepatitis than in the livers of the ivADSC group with normal livers (Fig. 5b). This result may suggest that the number of intravenously administered ADSCs that reached the liver was smaller in the chronic hepatitis model than in the normal liver model.

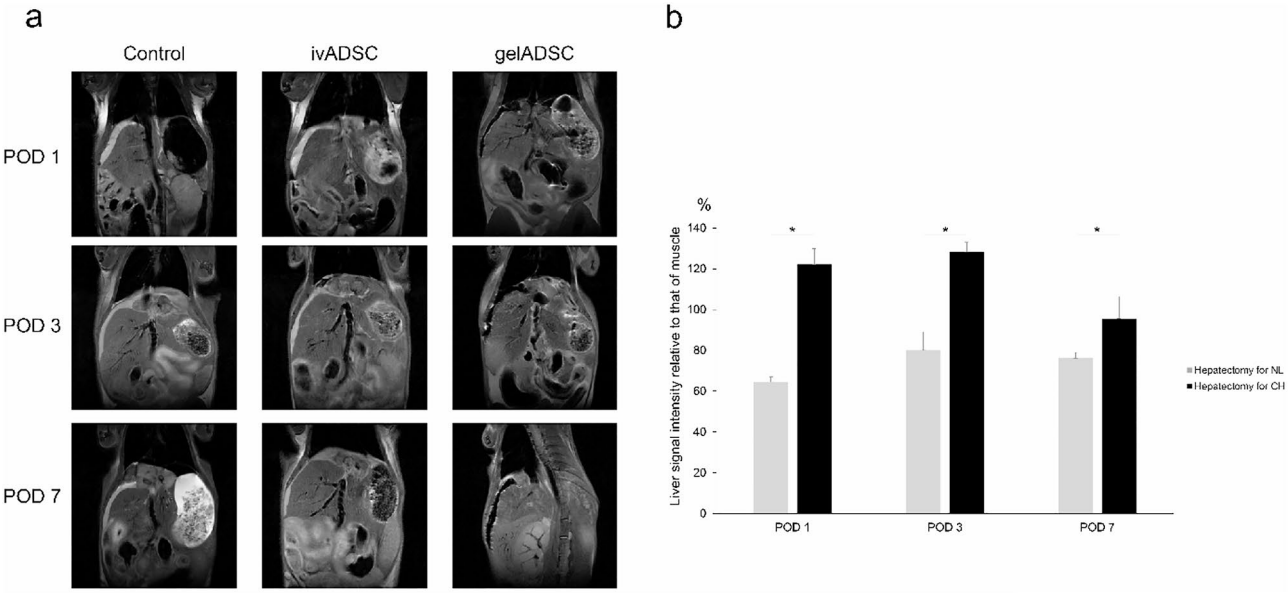

Fig. 5. MRI evaluation of ADSCs administered in a chronic hepatitis model. (**a**) The distribution of ADSCs administered in a chronic hepatitis model was evaluated by T2WI on PODs 1, 3, and 7. In the gelADSC group, fibrin gel exhibited low-intensity enhancement, reflecting the presence of ADSCs labeled with iron. In the ivADSC group, the distribution of intravenously administered ADSCs was not apparent. (**b**) The liver signal intensity relative to that of muscle was evaluated in the ivADSC groups with normal liver and with chronic hepatitis using the ImageJ software. The intensity was significantly lower in mice with hepatectomy and normal liver than in those with chronic hepatitis on POD 1, 3, and 7. $*p < 0.05$.

Extracellular vesicles play an important role in liver regeneration by gelADSC

Finally, we examined the impact of extracellular vesicles (EVs) released from ADSCs on the liver regeneration after hepatectomy. In in vitro experiments, ADSCs secreted more EVs when encapsulated in FG than when cultured without it, and EV secretion increased as time progressed (Fig. 6a; the uncropped membrane was shown in Supplementary Fig. S1). Blood samples from hepatectomized mice treated with gelADSC showed the presence of EV in serum from 8 to 16 h post-hepatectomy, persisting for at least 48 h (Fig. 6b; the uncropped membrane was shown in Supplementary Fig. S1). In this experiment, anti-CD63 antibody was used as an EV marker since this antibody does not have reactivity with mouse tissue. Subsequently, we inhibited ADSCs' EV secretion by siRNA-mediated knockdown of ALIX (referred to as $ADSC^{siALIX}$)[13]. The qPCR analysis confirmed the reduction of ALIX gene expression (Fig. 6c), and the attenuation of EV secretion was observed through reduced expression of EV markers such as TSG101 and syntenin in WB analysis (Fig. 6c; the uncropped membrane was shown in Supplementary Fig. S1). The secretion of cytokines, specifically HGF and SDF-1, by ADSCs was significantly reduced upon silencing ALIX mRNA, although the VEGF secretion remained unchanged (Fig. 6d). The impact of EVs on hepatectomy-induced liver regeneration was assessed using $gelADSC^{siALIX}$. The LTBR on POD 2 was significantly decreased in the $gelADSC^{siALIX}$ group relative to that in the $gelADSC^{siControl}$ group (mean: 0.035 vs. 0.038) (Fig. 6e). Moreover, the expression of Crot and Pparα mRNAs was significantly reduced in the $gelADSC^{siALIX}$ group (Fig. 6f). The findings suggest a significant contribution of EVs to post-hepatectomy liver regeneration, by upregulating the cell cycle and fatty acid oxidation along with the release of important cytokines.

Discussion

Our study demonstrated the promising therapeutic effects of direct ADSC administration in hepatectomized mice. One possible explanation for these positive outcomes is the paracrine effect of ADSCs. To obtain the paracrine effect, ADSCs must be administered in close proximity to the damaged tissue. For example, in animal models of bone or skin defects, tissue repair has been successfully achieved through local administration of ADSCs within a scaffold[14,15]. In the present study, we employed FG as a scaffold for ADSCs (gelADSC). The efficacy of FG as a scaffold for ADSCs has been previously reported. FG exhibits a durable mechanical structure, as evidenced by its stress-strain hysteresis loop properties[9]. Furthermore, FG has a three-dimensional porous structure, with pore diameters of approximately 1.69 μm[10]. This structural feature makes FG an ideal scaffold for ADSCs, as the diameter of ADSCs and ADSC-derived EVs is 10–25 μm[16] and 50–200 nm[17], respectively. FG can thus retain ADSCs while allowing the release of EVs. Moreover, FG provides uniform distribution and adhesion of ADSCs without inducing their differentiation into hepatocytes[8,11,18]. These characteristics make FG particularly suitable for maintaining the ADSCs' reparative capabilities, ensuring sustained delivery of paracrine factors to the injured tissue.

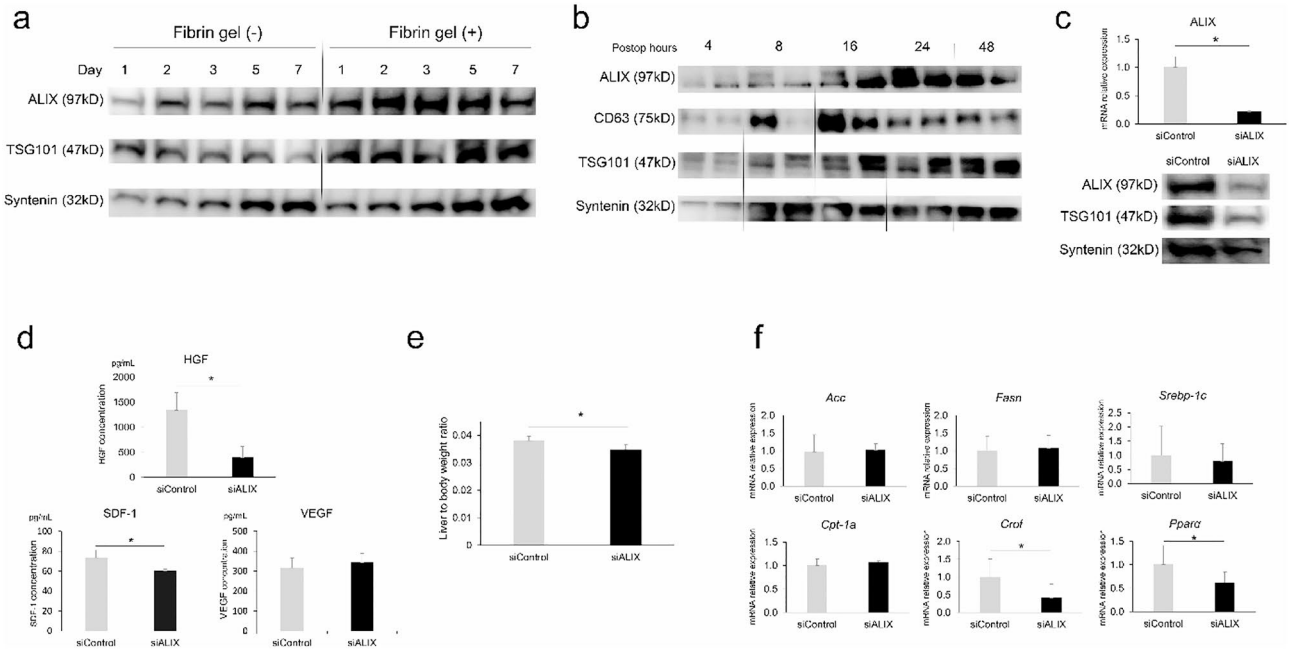

Fig. 6. Evaluation of the impact of extracellular vesicles (EVs) secreted from ADSCs. (**a**) EV secretion increased in a time-dependent manner, both with and without fibrin gel. Furthermore, EV secretion was higher with the use of fibrin gel compared with that in the absence of fibrin gel. (**b**) EV secretion was assessed using blood samples obtained from hepatectomized mice treated with gelADSC. EVs appeared in the serum from 8–16 h until at least 48 h post-hepatectomy. (**c**) EV secretion was inhibited by introducing ALIX-siRNA to ADSCs. The introduction of ALIX-siRNA was confirmed by PCR analysis, and it decreased the expression of the proteins TSG101 and syntenin. (**d**) The EV secretion of ADSC^{siControl} and ADSC^{siALIX} was compared. Although the VEGF concentrations were comparable, the concentrations of HGF and SDF-1 were significantly lower in ADSC^{siALIX}. (**e**) The therapeutic effect of gelADSC^{siALIX} was evaluated in a mouse hepatectomy model. The liver to body weight ratio at POD 2 was significantly decreased in the gelADSC^{siALIX} group. (**f**) mRNA expression in the liver was evaluated by real-time PCR. The expression of Acc, Fasn, Srebp-1c and Cpt-1a was comparable between the gelADSC^{siControl} group and the gelADSC^{siALIX} group, whereas that of Crot and Pparα was significantly reduced in the gelADSC^{siALIX} group. $^{*}p < 0.05$.

The therapeutic mechanism of gelADSC is summarized in Fig. 7. Our in vitro experiments showed continuous secretion of VEGF, HGF, and SDF-1, crucial for liver regeneration[19–21], for over 7 days when ADSCs were enclosed in FG. The crucial period for liver regeneration after hepatectomy is reported to be 7 days post-surgery[22], suggesting that gelADSC is an effective therapy for liver regeneration following liver resection. Additionally, increased HIF-1α expression was noted in gelADSC, which may contribute to the upregulated secretion of the cytokines, since hypoxic condition is associated with enhanced secretion of VEGF, HGF, and SDF-1[23–25]. Taking these results together, gelADSC presents a promising model for ADSCs' therapeutic effects on post-hepatectomy liver regeneration.

The therapeutic potential of gelADSC was subsequently assessed in vivo using a mouse hepatectomy model, revealing enhanced liver regeneration via upregulation of fatty acid oxidation and the cell cycle. Our results show that gelADSC contributed to lipolysis (i.e., fatty acid oxidation) rather than lipogenesis, consistent with a previous report[26]. The intravenous administration of ADSCs is a potent therapy for liver regeneration after hepatectomy of normal liver, despite the reports of entrapment by the lung[4,13]. Sid-Otmane et al. reported that intravenously administered ADSCs exert their therapeutic effect by an "endocrine-like" mechanism, where ADSCs trapped in the lung remotely function to repair damaged organs[27]. In the current study, the therapeutic impact of ivADSC was comparable to that of gelADSC. However, our MRI results showed that gelADSC and ivADSC showed different distribution of ADSCs. In the gelADSC group, ADSCs remained in FG on the surface of the liver for at least 7 days after hepatectomy, potentially enhancing their therapeutic effect. In contrast, in the ivADSC group, the MRI signal in the liver was enhanced at a comparatively low level for 7 days postoperatively. Previous studies suggested that intravenously administered ADSCs remain in liver for only 2 to 3 days[4], which seems contrary to our MRI findings. However, we need to be cautious in the interpretation of MRI because the presence of ADSCs was indirectly evaluated as the presence of iron. Moreover, although gelADSC was a potent method to administer ADSCs in the setting of hepatectomy, other administration routes, such as injection into a portal system, still warrant future studies to further evaluate the efficacy of gelADSC. Overall, gelADSC exhibited a therapeutic effect, promoting liver regeneration via fatty acid oxidation and cell cycle, and ivADSC also displayed comparably potent effects in normal liver hepatectomy models.

The therapeutic effect of gelADSC was also evaluated in mice with underlying chronic hepatitis because, in current surgical practice, approximately 54% of the patients undergoing hepatectomy have chronic hepatitis[28].

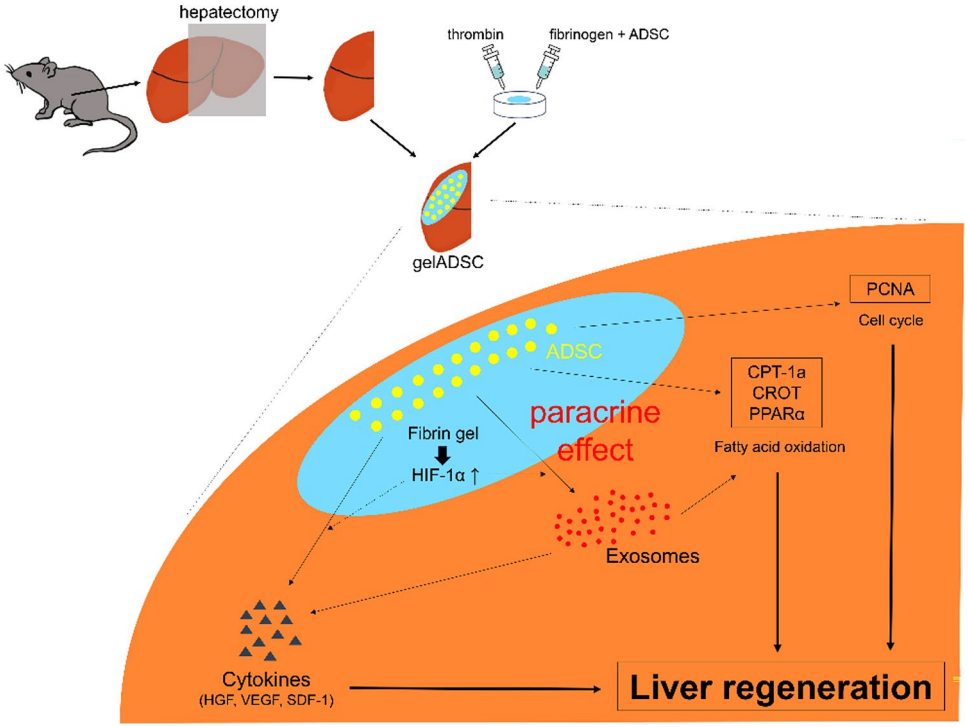

Fig. 7. The therapeutic mechanism of gelADSC. GelADSC contributed to liver regeneration post-hepatectomy through the upregulation of cytokine secretion, fatty acid oxidation, and cell cycle. In particular, extracellular vesicles released from ADSCs were significantly associated with cytokine secretion and fatty acid oxidation.

In a mouse model of underlying chronic hepatitis, gelADSC demonstrated significant upregulation of fatty acid oxidation and cell cycle compared not only to the control group but also probably to the ivADSC group. Interestingly, our MRI findings indicate that the distribution of intravenously administered ADSCs differed according to the presence or absence of underlying chronic hepatitis. Specifically, fewer ADSCs reached the liver in the chronic hepatitis model compared to the normal liver model. This discrepancy may explain why ivADSC might show inferior therapeutic potential to gelADSC in the chronic hepatitis model, unlike in the normal liver model. Therefore, especially in patients with chronic hepatitis, gelADSC could be a preferable therapeutic option for liver regeneration post-hepatectomy potentially over ivADSC.

EVs have been considered crucial to liver regeneration by gelADSC. Hypoxia has been reported to promote the secretion of EVs[29]. Our study found that ADSCs secrete significantly more EVs when embedded in FG (Fig. 6a), suggesting the hypoxic environment in FG favored EV release. Interestingly, EVs appeared in the serum of hepatectomized mice treated with gelADSC from 8 to 16 h until at least 48 h after surgery (Fig. 6b). A previous report described that, when ADSCs were intravenously administered, the amount of serum EV markedly increased at 4 h after administration, rapidly decreasing thereafter[13]. The continuous release of EVs from gelADSC may have contributed to enhanced liver regeneration after hepatectomy. Moreover, inhibiting the release of EVs from ADSC in vivo led to a significant decrease in HGF and SDF-1 secretion in vitro, reduced LTBR levels, and downregulated mRNA levels related to fatty acid oxidation. This underscores the therapeutic role of EVs in gelADSC. Indeed, the concept of using EVs instead of ADSCs has already been reported, due to EVs' lack of immunogenicity[30]. Nevertheless, the application of gelADSC led to a time-dependent and persistent increase in EV secretion (Fig. 6a), offering a clinical advantage in liver regeneration post-hepatectomy.

In clinical scenarios like living-donor liver transplantation, gelADSC holds promise beyond post-hepatectomy use. Addressing concerns like small-for-size syndrome[31], administering gelADSC to the grafted liver could facilitate liver regeneration. Although a large area must be covered by gelADSC, considering the size of the human liver, Mori et al.'s cell spray method[6] offers a potential solution. This technique, previously used to spray FG onto the heart, ensures consistent distribution on the liver surface.

The current study has some limitations. First, due to the use of ADSCs of human origin, the therapeutic potential of gelADSC as an allograft or autograft was not evaluated. Second, the absence of an adequate control group to compare the gelADSC and the ivADSC groups makes us cautious in interpreting the results of this comparison. Third, the validity of using TAA to induce chronic hepatitis is controversial. The pathogenesis of chronic hepatitis in human beings is quite different. Finally, we need to be careful in interpreting MR images. It remains unclear how long ADSCs can retain iron after being administered in vivo.

In conclusion, the therapeutic effect of ADSCs' direct administration in the post-hepatectomy setting was validated using FG as a scaffold, highlighting their superiority over intravenously administered ADSCs, particularly in the context of underlying chronic hepatitis.

Methods

Human ADSCs and FG preparation

Human ADSCs of fourth passage (Lonza Japan, Tokyo) were cultured at 37 °C in a 5% CO_2 atmosphere for a few days. FG was purchased from CSL Behring (King of Prussia, PA, USA).

Assessment of cytokine secretion and survival of ADSCs in FG

In preparation of gelADSC, 1.0×10^6 ADSCs were mixed with 100 µL of 2-fold diluted fibrinogen concentrate. Subsequently, 100 µL of 2-fold diluted thrombin concentrate was added to the mixture of ADSCs and fibrinogen. First, to assess the ADSCs' survival within FG, gelADSC was cultured for 7 days in DMEM (high glucose) with 2% FBS. After formalin fixation, gelADSC was paraffin-embedded for H&E staining to evaluate morphology. TUNEL staining was utilized to assess the proportion of viable cells using an apoptosis kit (Medical Biological Lab, Nagoya, Japan). Optical microscopy (Keyence, Osaka, Japan) was used for examination of the images.

Furthermore, we evaluated the dynamics of cytokine secretion by gelADSC by culturing it in high-glucose DMEM containing 2% FBS until day 7. No medium change was performed during the incubation period. Supernatants were collected at five time points (days 1, 2, 3, 5, and 7). The control group consisted of ADSCs dispersed in high-glucose DMEM containing 2% FBS without the use of FG and underwent the same collection. The concentrations of VEGF, HGF, and SDF-1 per 1.0×10^5 ADSCs in the supernatants were evaluated by ELISA (Abcam). Then, to assess the unique environment within the FG, WB analysis of HIF-1α (Abcam) was performed using the samples obtained on days 3, 5, and 7.

Mouse hepatectomy models and ADSC administration

This study was approved by the Animal Experiments Committee, Osaka University (approval number 03-001-003). Animal care was in accordance with institutional guidelines. The animal studies were conducted in accordance with the ARRIVE guidelines. Male 7-week-old C57BL/6 mice, which were purchased from Clea Japan (Tokyo, Japan), were acclimatized for 1 week before experiments and housed with a 12-hour dark/light cycle.

A 70% partial hepatectomy was performed as previously described, with the mice under general anesthesia using medetomidine, midazolam, and butorphanol[32]. In the gelADSC group ($n = 5$), FG containing 1.0×10^6 ADSCs was attached to the remnant liver surface immediately after liver resection, whereas in the control group ($n = 5$), FG not containing ADSCs was placed on the remnant liver. In this study, the ivADSC group was prepared to evaluate the therapeutic effect of gelADSC in comparison with a conventional method to administer ADSCs. In the ivADSC group ($n = 5$), FG without ADSCs was placed on the liver and 1.0×10^6 ADSCs were dissolved in 100 µL of HBSS solution (Thermo Fisher Scientific, MA, USA) and were injected into a tail vein. 90% partial hepatectomy was performed as a fatal hepatic failure model[33]. In this model, the survival of the mice was examined every 6 hours and compared between the gelADSC group ($n = 16$) and the control group ($n = 16$).

We also evaluated the effect of gelADSC on liver with chronic hepatitis. The mice were injected intraperitoneally with 150 mg/kg TAA twice a week for 5 weeks in accord with our previous report[34]. The liver fibrosis induced by TAA was confirmed by staining with Masson trichrome. A 70% partial hepatectomy was performed 2 to 3 days after the final TAA administration.

In each hepatectomy model, the liver and serum samples were collected and assessed at several time points. LTBR was measured after removing FG from the liver in order to exclude the weight of FG from the final measurements.

Cholesterol and triglyceride assays

Lipid was extracted from a mouse liver sample by the method of Folch et al.[35]. Triglyceride and cholesterol levels were measured using a LabAssay Triglyceride kit (Fujifilm Wako Shibayagi Corp., Gunma, Japan) and LabAssay Cholesterol kit (Fujifilm Wako Shibayagi Corp.), respectively, according to the manufacturer's protocol.

Iron labeling and MRI evaluation

ADSCs were labeled with iron by overnight incubation in high-glucose DMEM containing ferucarbotran (25 µg Fe/mL) and poly-L-lysine (0.75 mg/mL)[36]. The iron labeling was confirmed by Berlin blue staining. The iron-labeled ADSCs administered to mice were detected using 7T- MRI. All MRI experiments were performed on a horizontal 7T-MRI (PharmaScan 70/16 US, Bruker BioSpin, Ettlingen, Germany) equipped with a volume coil with a 30-mm inner diameter. T2WI was obtained with rapid acquisition with a relaxation enhancement (RARE) sequence. The sequence parameters were as follows: repetition time (TR) = 2300 ms, echo time (TE) = 33 ms, the field of view (FOV) = 25.6×25.6 mm^2, slice thickness = 1 mm, matrix size = 128×128, the number of averages = 1, and in-plane resolution = 200×200 µm^2. The relative liver intensity on MRI was evaluated by dividing liver intensity by muscle intensity (Supplementary Fig. S4).

EV isolation from cell culture supernatants and mouse blood samples

EVs were isolated from cell culture supernatants and mouse blood samples as described previously[37]. The existence of EVs was confirmed by the use of WB to demonstrate the upregulated expression of several markers associated with EVs, including syntenin, TSG101, and ALIX (Abcam). First, we investigated the impact of FG on the secretion of EVs from ADSCs. 1.0×10^5 ADSCs were incubated with or without FG for 7 days using high-glucose DMEM containing 2% FBS, and the culture supernatant was collected on days 1, 2, 3, 5, and 7. Next, we evaluated the impact of EVs on liver regeneration after hepatectomy by inhibiting EV release from ADSCs. A previous study reported that introducing ALIX-siRNA to ADSCs can inhibit their EV secretion[13]. The successful introduction of ALIX-siRNA (ADSCs^{siALIX}) was confirmed by qPCR analysis and WB analysis. ADSCs^{siALIX} were cultured for 48 h in Mesenchymal Stem Cell Growth Medium 2 (PromoCell, Heidelberg, Germany). After

a 48-hour incubation, the supernatant was subjected to ELISA analysis to evaluate cytokine secretion, and the cells (ADSCs^{siALIX}) were embedded in FG (gelADSC^{siALIX}) and administered to 70%-hepatectomy model mice.

RT-PCR
Total RNA extraction and real-time RT-PCR was performed in accordance with our previous report[34]. Relative expression levels of mRNAs were determined as the ratio of specific mRNA to endogenous glyceraldehyde-3-phosphate dehydrogenase (GAPDH) mRNA. The primers used in the experiments are listed in Supplementary Table S1.

Western blot analysis
Total protein extracts were obtained in accordance with our previous report[34]. The primary antibodies included anti-HIF-1α, ALIX, TSG101, syntenin (Abcam), and CD63 (BD Biosciences), as well as an anti-β actin antibody (Sigma-Aldrich, Tokyo, Japan). The detection of the antigen–antibody complex was achieved using an ECL Prime Western Blotting Detection kit (GE Healthcare).

Histological analysis
The paraffin-embedded sections were stained with H&E or Masson's trichrome, or were subjected to immunohistochemical labeling using antibodies for PCNA (Cell Signaling Technology [CST]), CD90 (CST), CD105 (Proteintech), hepatocyte-specific antigen (CST), and arginase-1 (CST) along with an LSABTM kit, a system for automated labeled streptavidin–biotinylated antibody immunostaining (both from DAKO, Glostrup, Denmark).

Statistical analysis
The data are presented as mean ± SDs. The means of continuous variables were compared using Student's t test or analysis of variance followed by Tukey's test. P-values < 0.05 were considered significant. All statistical analyses were calculated with JMP software (JMP, version 13.2.1).

Data availability
The datasets generated during and/or analyzed during the current study are available from the corresponding author on reasonable request.

Received: 22 July 2024; Accepted: 17 February 2025
Published online: 21 February 2025

References
1. Søreide, J. A. & Deshpande, R. Post hepatectomy liver failure (PHLF) - recent advances in prevention and clinical management. *Eur. J. Surg. Oncol.* **47**, 216–224. https://doi.org/10.1016/j.ejso.2020.09.001 (2021).
2. Cai, Y., Li, J., Jia, C., He, Y. & Deng, C. Therapeutic applications of adipose cell-free derivatives: a review. *Stem Cell Res. Ther.* https://doi.org/10.1186/s13287-020-01831-3 (2020).
3. Papanikolaou, I. G. et al. Mesenchymal Stem cells transplantation following partial hepatectomy: A new concept to promote liver regeneration-systematic review of the literature focused on experimental studies in rodent models. *Stem Cells Int* 7567958. https://doi.org/10.1155/2017/7567958 (2017).
4. Watanabe, Y. et al. Mesenchymal stem cells and Induced Bone Marrow-Derived macrophages synergistically improve liver fibrosis in mice. *STEM CELLS Translational Med.* **8**, 271–284. https://doi.org/10.1002/sctm.18-0105 (2019).
5. Jung, J. W. et al. Familial occurrence of Pulmonary Embolism after Intravenous, adipose tissue-derived stem cell therapy. *Yonsei Med. J.* **54**, 1293. https://doi.org/10.3349/ymj.2013.54.5.1293 (2013).
6. Mori, D. et al. Cell spray transplantation of adipose-derived mesenchymal stem cell recovers ischemic cardiomyopathy in a Porcine Model. *Transplantation* **102**, 2012–2024. https://doi.org/10.1097/tp.0000000000002385 (2018).
7. Hu, C., Zhao, L. & Li, L. Current understanding of adipose-derived mesenchymal stem cell-based therapies in liver diseases. *Stem Cell Res. Ther.* https://doi.org/10.1186/s13287-019-1310-1 (2019).
8. Wu, X., Ren, J. & Li, J. Fibrin glue as the cell-delivery vehicle for mesenchymal stromal cells in regenerative medicine. *Cytotherapy* **14**, 555–562. https://doi.org/10.3109/14653249.2011.638914 (2012).
9. Sawadkar, P. et al. Three dimensional porous scaffolds derived from collagen, elastin and fibrin proteins orchestrate adipose tissue regeneration. *J. Tissue Eng.* **12**, 20417314211019238. https://doi.org/10.1177/20417314211019238 (2021).
10. Moreno-Arotzena, O., Meier, J., Del Amo, C. & García-Aznar, J. Characterization of fibrin and Collagen Gels for Engineering Wound Healing models. *Materials* **8**, 1636–1651. https://doi.org/10.3390/ma8041636 (2015).
11. Bagheri-Hosseinabadi, Z., Salehinejad, P. & Mesbah-Namin, S. A. Differentiation of human adipose-derived stem cells into cardiomyocyte-like cells in fibrin scaffold by a histone deacetylase inhibitor. *Biomed. Eng. Online*. https://doi.org/10.1186/s12938-017-0423-y (2017).
12. Wells, C. I. et al. Haemostatic efficacy of Topical agents during Liver Resection: A Network Meta-Analysis of Randomised trials. *World J. Surg.* **44**, 3461–3469. https://doi.org/10.1007/s00268-020-05621-z (2020).
13. Nakamura, Y. et al. Adiponectin stimulates Exosome Release to enhance mesenchymal stem-cell-driven therapy of Heart failure in mice. *Mol. Ther.* **28**, 2203–2219. https://doi.org/10.1016/j.ymthe.2020.06.026 (2020).
14. Lee, J. et al. Osteogenesis of adipose-derived and bone marrow stem cells with Polycaprolactone/Tricalcium phosphate and three-dimensional Printing Technology in a dog model of Maxillary Bone defects. *Polymers* **9**, 450. https://doi.org/10.3390/polym9090450 (2017).
15. Nishiwaki, K. et al. In situ transplantation of adipose tissue-derived stem cells organized on porous polymer nanosheets for murine skin defects. *J. Biomed. Mater. Res. Part. B* **107**, 1363–1371. https://doi.org/10.1002/jbm.b.34228 (2019).
16. Bora, P. & Majumdar, A. S. Adipose tissue-derived stromal vascular fraction in regenerative medicine: a brief review on biology and translation. *Stem Cell Res. Ther.* https://doi.org/10.1186/s13287-017-0598-y (2017).
17. Sun, D. et al. High yield engineered nanovesicles from ADSC with enriched mir-21-5p promote angiogenesis in adipose tissue regeneration. *Biomater. Res.* **26**, 83. https://doi.org/10.1186/s40824-022-00325-y (2022).
18. Bhang, S. H. et al. Mutual effect of subcutaneously transplanted human adipose-derived stem cells and pancreatic islets within fibrin gel. *Biomaterials* **34**, 7247–7256. https://doi.org/10.1016/j.biomaterials.2013.06.018 (2013).

19. Ross, M. A., Sander, C. M., Kleeb, T. B., Watkins, S. C. & Stolz, D. B. Spatiotemporal expression of angiogenesis growth factor receptors during the revascularization of regenerating rat liver. *Hepatology* **34**, 1135–1148. https://doi.org/10.1053/jhep.2001.29624 (2001).
20. Ishikawa, T. et al. Hepatocyte growth factor/c-met signaling is required for stem-cell-mediated liver regeneration in mice. *Hepatology* **55**, 1215–1226. https://doi.org/10.1002/hep.24796 (2012).
21. Ding, B. S. et al. Divergent angiocrine signals from vascular niche balance liver regeneration and fibrosis. *Nature* **505**, 97–102. https://doi.org/10.1038/nature12681 (2014).
22. Duncan, A. W., Dorrell, C. & Grompe, M. Stem cells and liver regeneration. *Gastroenterology* **137**, 466–481. https://doi.org/10.1053/j.gastro.2009.05.044 (2009).
23. Kim, K. J. et al. Inhibition of vascular endothelial growth factor-induced angiogenesis suppresses tumour growth in vivo. *Nature* **362**, 841–844. https://doi.org/10.1038/362841a0 (1993).
24. Pennacchietti, S. et al. Hypoxia promotes invasive growth by transcriptional activation of the met protooncogene. *Cancer Cell.* **3**, 347–361. https://doi.org/10.1016/s1535-6108(03)00085-0 (2003).
25. Ceradini, D. J. et al. Progenitor cell trafficking is regulated by hypoxic gradients through HIF-1 induction of SDF-1. *Nat. Med.* **10**, 858–864. https://doi.org/10.1038/nm1075 (2004).
26. Wang, J. L., Ding, H. R., Pan, C. Y., Shi, X. L. & Ren, H. Z. Mesenchymal stem cells ameliorate lipid metabolism through reducing mitochondrial damage of hepatocytes in the treatment of post-hepatectomy liver failure. *Cell Death Dis.* https://doi.org/10.1038/s41419-020-03374-0 (2021).
27. Sid-Otmane, C., Perrault, L. P. & Ly, H. Q. Mesenchymal stem cell mediates cardiac repair through autocrine, paracrine and endocrine axes. *J. Translational Med.* https://doi.org/10.1186/s12967-020-02504-8 (2020).
28. Nakano, M. et al. Trends in hepatocellular carcinoma incident cases in Japan between 1996 and 2019. *Sci. Rep.* https://doi.org/10.1038/s41598-022-05444-z (2022).
29. Bister, N. et al. Hypoxia and extracellular vesicles: a review on methods, vesicular cargo and functions. *J. Extracell. Vesicles*. **10**, e12002. https://doi.org/10.1002/jev2.12002 (2020).
30. Keshtkar, S., Azarpira, N. & Ghahremani, M. H. Mesenchymal stem cell-derived extracellular vesicles: novel frontiers in regenerative medicine. *Stem Cell Res. Ther.* https://doi.org/10.1186/s13287-018-0791-7 (2018).
31. Gao, W. et al. Adipose-derived mesenchymal stem cells promote liver regeneration and suppress rejection in small-for-size liver allograft. *Transpl. Immunol.* **45**, 1–7. https://doi.org/10.1016/j.trim.2017.07.005 (2017).
32. Mitchell, C. & Willenbring, H. A reproducible and well-tolerated method for 2/3 partial hepatectomy in mice. *Nat. Protoc.* **3**, 1167–1170. https://doi.org/10.1038/nprot.2008.80 (2008).
33. Makino, H. et al. A good model of hepatic failure after excessive hepatectomy in mice. *J. Surg. Res.* **127**, 171–176. https://doi.org/10.1016/j.jss.2005.04.029 (2005).
34. Toya, K. et al. Efficacy of autologous skeletal myoblast cell sheet transplantation for liver regeneration in liver failure. *Transplantation* https://doi.org/10.1097/tp.0000000000004567 (2023).
35. Folch, J., Lees, M. & Sloane Stanley, G. H. A simple method for the isolation and purification of total lipides from animal tissues. *J. Biol. Chem.* **226**, 497–509 (1957).
36. Noorwali, A., Faidah, M., Ahmed, N. & Bima, A. Tracking iron oxide labelled mesenchymal stem cells(MSCs) using magnetic resonance imaging (MRI) in a rat model of hepatic cirrhosis. *Bioinformation* **15**, 1–10. https://doi.org/10.6026/97320630015001 (2019).
37. Obata, Y. et al. Adiponectin/T-cadherin system enhances exosome biogenesis and decreases cellular ceramides by exosomal release. *JCI Insight*. https://doi.org/10.1172/jci.insight.99680 (2018).

Acknowledgements

This study was supported by diligent staff at the Center for Medical Research and Education and the Center of Medical Innovation and Translational Research, Graduate School of Medicine, Osaka University. This study was funded by Rohto Pharmaceutical Co., Ltd.

Author contributions

HI, YT, SK (Shogo Kobayashi), and HE have made substantial contributions to the conception of the work; HI, AH, and SS to the acquisition and analysis of the data; HI, YT, SK (Shogo Kobayashi), SK (Shunbun Kita), KS, YI, DY, TN, HT, DH, TK, and KT to the interpretation of the data; and HI, YT, TK, SS, IS, SM, YD, and HE to drafting and revising the manuscript.

Funding

This study was funded by Rohto Pharmaceutical Co., Ltd.

Declarations

Competing interests

HI received a research fund from Rohto Pharmaceutical Co., Ltd., and SK (Shogo Kobayashi) received honoraria from AstraZeneca and Taiho. The other authors (YT, AH, SK (Shunbun Kita), KS, YI, DY, TN, HT, DH, TK, KT, TK, SS, IS, SM, YD, HE) declare no competing financial interests.

Additional information

Supplementary Information The online version contains supplementary material available at https://doi.org/10.1038/s41598-025-90805-7.

Correspondence and requests for materials should be addressed to S.K.